22

Jiangjia Ravine debris flows in south-western China

Peng Cui, Xiaoqing Chen, Yuyi Waqng, Kaiheng Hu, and Yong Li

22.1 INTRODUCTION

China is a mountainous country. More than 6.4×10^6 km^2 of the territory consists of complex, tectonically active terrain with a monsoon climate within which debris flows are common and create huge losses every year. Debris-flow activity is concentrated in the west and north-east parts of the mainland, including the provinces of Beijing, Sichuan, Yunnan, Xinjiang, Gansu, Xizang, as well as in Taiwan (Figure 22.1). There are about 50,000 debris-flow sites distributed over 48% of the territory area, threatening or damaging 138 central cities, 1,200 towns and villages, 36 railways, 50,000 km of highways, 1,200 km^2 of farmland, and many mines. River navigation and some large reservoirs, potentially including the Three Gorges Reservoir, are adversely affected by debris-flow sediment. The annual losses from debris flows approach US$ 366 million, and the annual death toll exceeds 100 (Tang et al., 2000). Debris-flow activity also increases soil erosion and ecological degradation, severely restricting the economic development of mountainous areas.

The majority of debris flows in China are triggered by rainfall. The Jiangjia Ravine in Yunnan Province has attracted global attention for the annual occurrence of well-documented episodes of rainfall-triggered debris flows. The site has an unparalleled record of long-term observations and experiments of the Dongchuan Debris Flow Observation and Research Station (DDFORS), a facility of the Institute of Mountain Hazards and Environment, Chinese Academy of Science. Debris flows in Jiangjia Ravine are typical of those in most mountainous areas of China and exhibit a variety of flow types, patterns, and processes under natural conditions. Chinese scientists have studied flow formation, static and dynamic properties, and deposition, and have attempted forecasting, warning, and mitigation of debris flows in Jiangjia Ravine for many years. In this chapter, we summarize some key findings from nearly four decades of data collection and research at the site.

M. Jakob and O. Hungr (eds), *Debris-flow Hazards and Related Phenomena*.

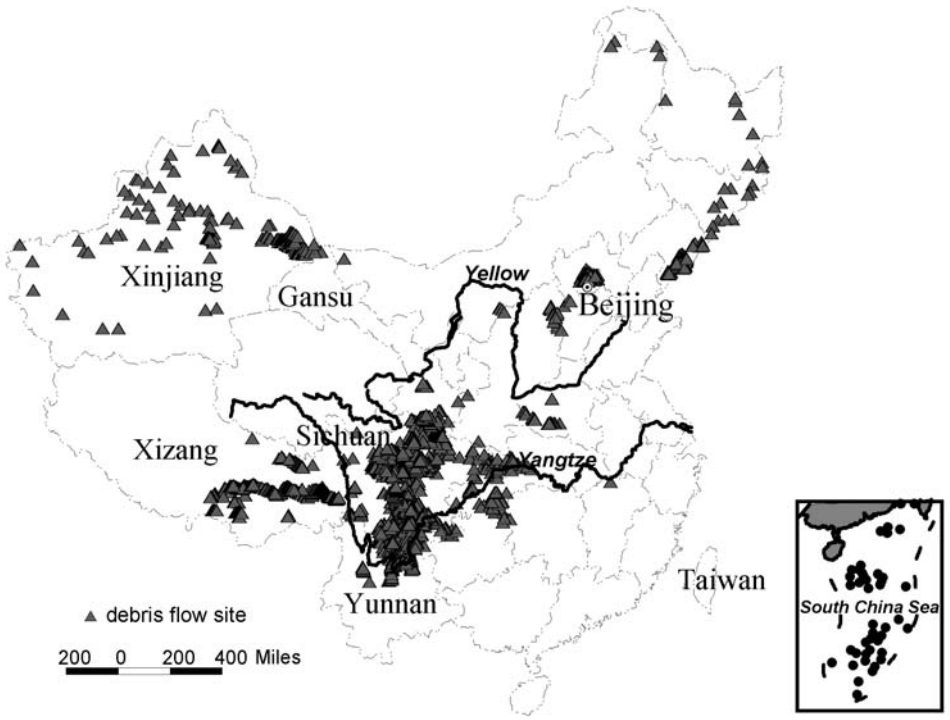

Figure 22.1. Map of debris flows distribution in China.

Jiangjia Ravine watershed with an area of 48.6 km^2 between N26°13′∼N26°17′ and E103°06′∼E103°13′, is located in the northern part of the Yunnan-Guizhou Plateau. The drainage joins the Xiaojiang River 31 km south of the confluence of the Xiaojiang and Jinsha Rivers. The main channel of the Jiangjia Ravine extends from the drainage divide at 3,269 m altitude west to the junction with the Xiaojiang at 1,042 m (Figure 22.2). Slopes steeper than 25° comprise 55% of the basin area with typical local relief of 500 m (Figure 22.3) (Wu et al., 1990). The basin consists of 5 orders of sub-basins (shown in Table 22.1), where the sum of all stream lengths is 124 km, and the stream density is 2.6 km/km^2. The main channel can be divided into three sections with different morphologic characteristics (Figure 22.4): (1) the erosion section, 10 km in length and 17° of bed slope on average; (2) the debris-flow transport section, 1.3 km in length and 5.1° of bed slope on average, with great cross-sectional variation up to 16 m in depth caused by scouring and silting of debris flows; and (3) the deposition section, 4.2 km in length and 3.7° bed slope on average. Table 22.1 shows the detailed characteristics of the ravine.

The Jiangjia Ravine has developed in the zone of the Xiaojiang fault, of which two branches join in the downstream reaches. The area is characterized by intense tectonism. About 80% of the exposed rocks are highly fractured and mildly metamorphosed. The sandstone and slate can be grouped into two types by color, both of

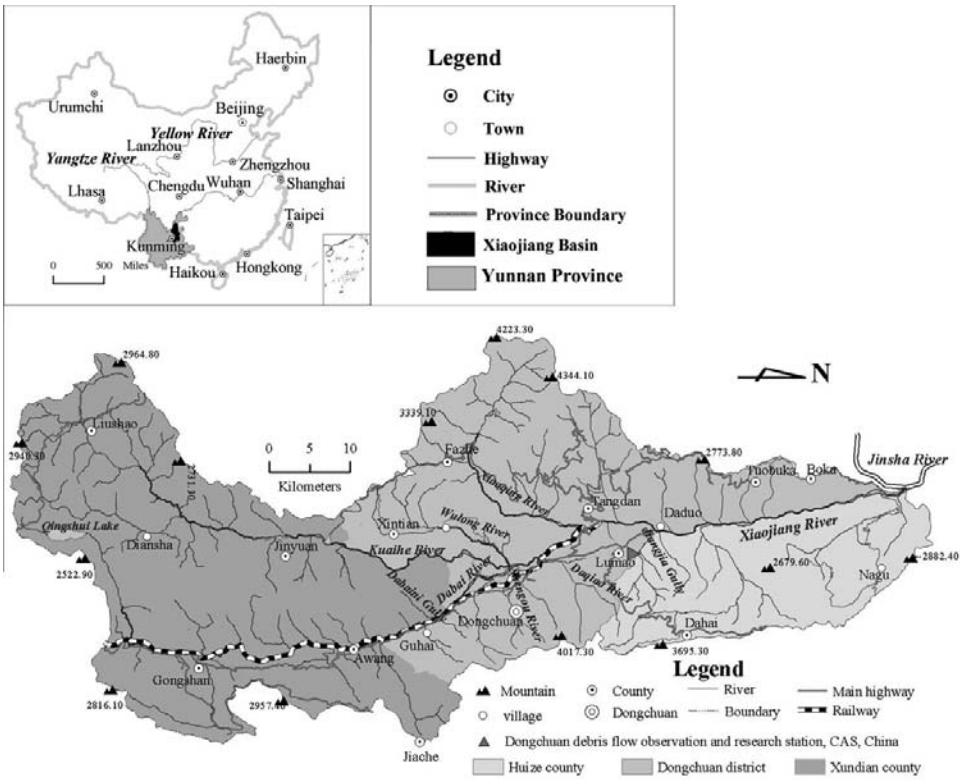

Figure 22.2. Location of Jiangjia Ravine.
From He (2003).

which are weak and easily weathered and broken into fragments. Colluvium and mantlerock are widely distributed on slopes and in channels in some sub-basins. The total volume of accumulated clastic detritus as source material for debris flows is estimated to $1.2 \times 10^9\,\mathrm{m}^3$ (Li and Wu, 1980).

Annual rainfall in the Jiangjia Ravine ranges from 400–1,000 mm and is markedly seasonal. About 85% of the total annual rain occurs between May and October. About 40% rainfall occurs between altitudes of 2,500 m and 3,000 m, but within an area of only 10% of the total watershed. Reflecting both the climate and human activity, the ground cover consists of: forest 4.2%, shrub land 8.4%, grassland 26.9%, and barren terrain 26.3%, while the other 34.2% includes alluvial surfaces and fans, farmland, and other land uses.

These conditions provide an ideal setting for recurrent debris flows. Since 1965, more than 400 episodes of debris-flow activity have occurred, each consisting of many individual surges. As many as 28 episodes have occurred in a single year. Annual sediment yielded in the Jiangjia Ravine is $2.0 \times 10^6\,\mathrm{m}^3$ on average while a maximum of $6.6 \times 10^6\,\mathrm{m}^3$ occurred in 1991.

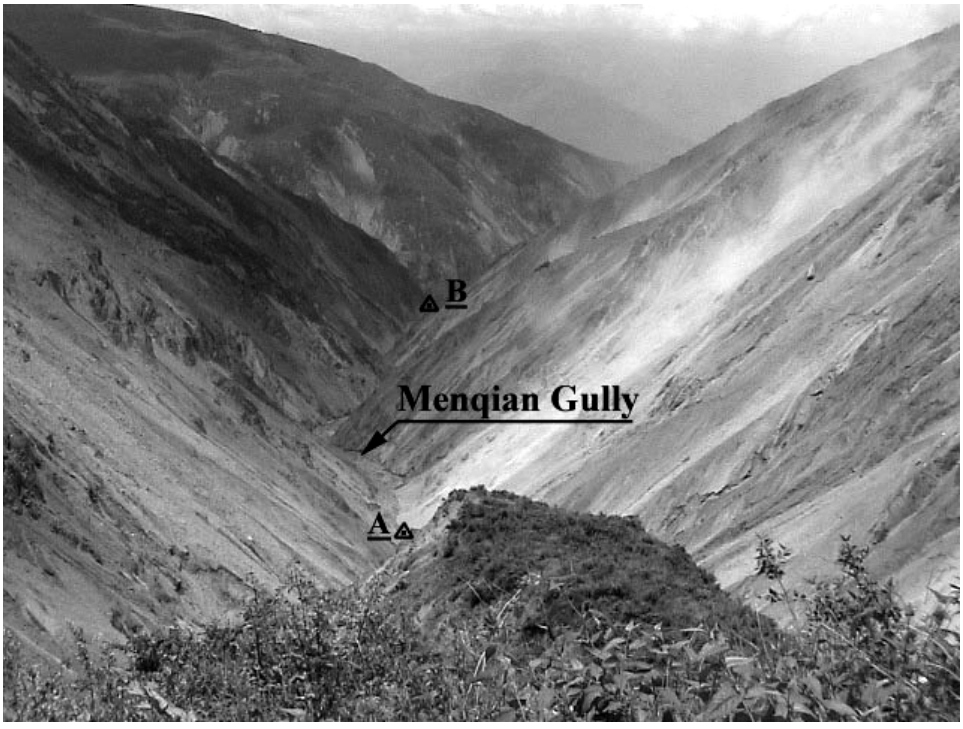

Figure 22.3. Debris-flow source region of Jiangjia Ravine (Point A is upstream of the Menqian Gully and Point B is the confluence point of the Menqian Gully and the Duozhao Gully, also shown in Figure 22.4. The length from A to B is 2.2 km.)
Photo: Hu, K.H. on 12 July 2001.

Table 22.1. Morphologic characteristics of the Jiangjia Ravine.
From Wu et al. (1990).

	Streams			Debris deposited sections		
Order	%	Length (km)	Slope (°)	%	Length (km)	Slope (°)
I	62.5	77.5	31.8	5.1	1.4	29.7
II	15.8	19.6	23.6	18.9	5.2	12.4
III	11.1	13.8	13.3	17.1	4.7	9.6
IV	4.5	5.6	9.5	36.4	10	7
V	6.1	7.5	4.5	22.5	6.2	3.7
Total	*100*	*124*	–	*100*	*27.5*	–

% = percentage of total watershed area of each sub-watershed order.

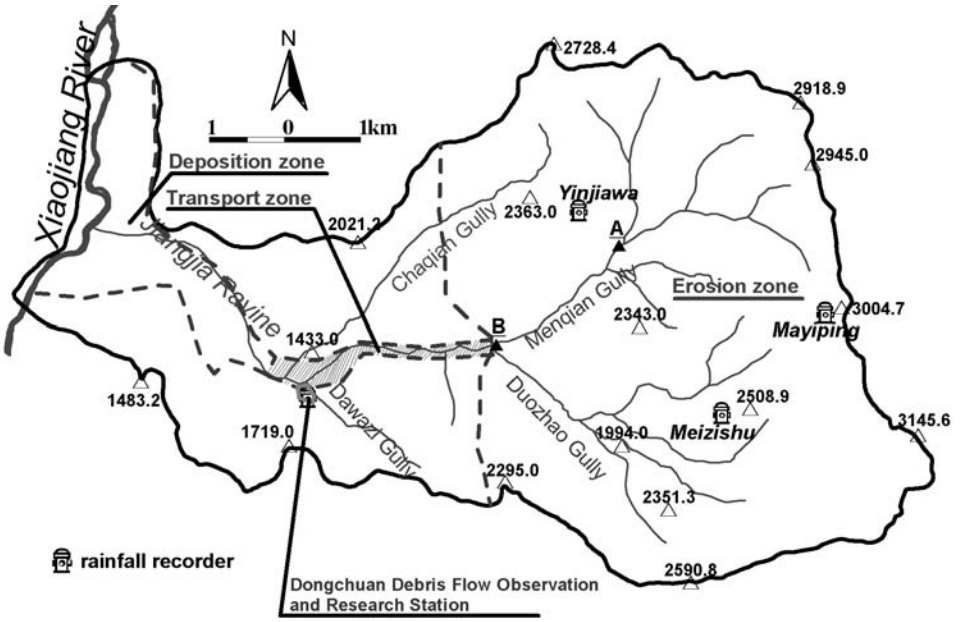

Figure 22.4. Plane view of Jiangjia Ravine. (The number in the figure is an elevation value. Point A and B are the same as the two in Figure 22.3.)

22.2 RELATIONSHIPS BETWEEN RAINFALL AND DEBRIS FLOW

Water is a necessary agent for debris-flow movement through liquefying and mobilizing loose detritus. In the Jiangjia Ravine rainfall is the main source of water while minor sources include snowfall and hail. DDFORS instrumentation in the Jiangjia Ravine includes four rain gauges at different elevations in the watershed. One is located at Mayiping, where debris flows originate; the others are at Meizishu, Yinjiawa, and the station (Figure 22.4). They provide data with which to analyse the relationships between precipitation and debris flow. For example, from 24 July to 8 July 2001, there were only two days with no rainfall but five days with rainfall in excess of 20 mm. The total amount of rainfall over 15 days was 246.7 mm recorded by the gauge at Mayiping (Figure 22.5). Antecedent rainfall saturated loose materials in the source, facilitating the initiation of debris flow. Debris flows occurred in the observations station in the erosion section at about 7:00 on 8 July, after rainfall began at 22:00 on the preceding day and increased abruptly at 6:20 on 8 July. Peak rainfall intensity of 10.8 mm/hr occurred at 8:20, followed by the maximal debris-flow discharge (775.2 m^3/s) at 9:25. Three periods of intense rainfall occurred until 20:20, when the rainfall ended (Figure 22.5). Peak debris-flow activity did not occur until intense rainfall occurred in the middle and downstream reaches (Wei et al., 2002).

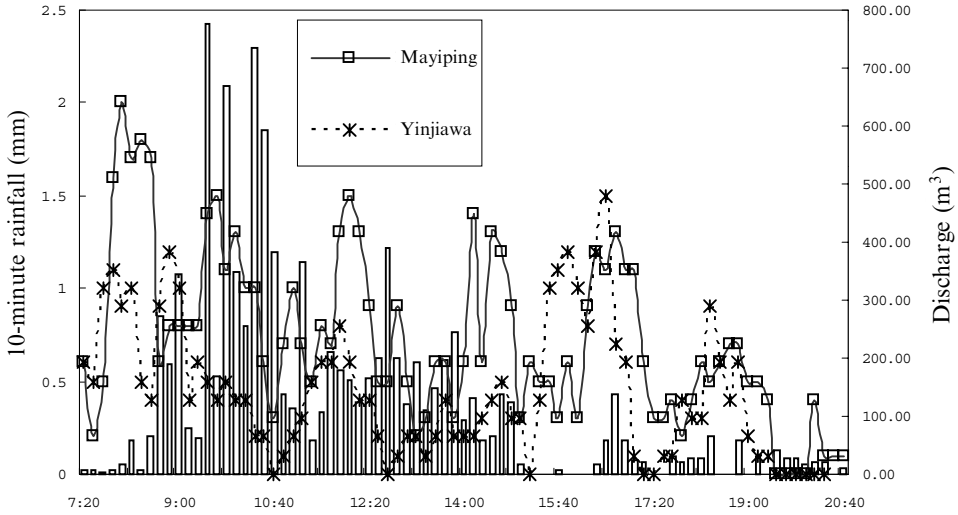

Figure 22.5. 10-min rainfall and debris flow of discharge on 8 July 2001, in the Jiangjia Ravine.

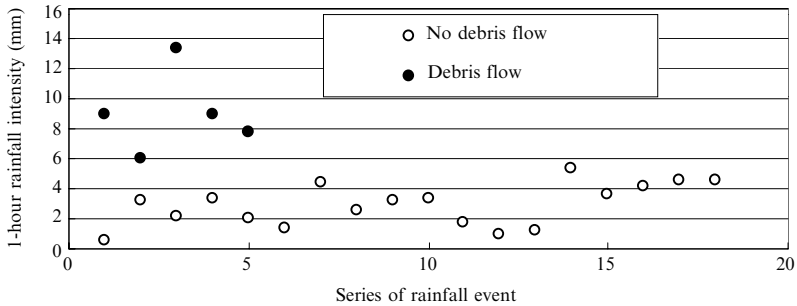

Figure 22.6. 1-hr rainfall intensity and related debris flows.

A single episode of debris flow is usually affected by both antecedent rainfall and concurrent rainfall. The 1-hr rainfall intensity is crucial, as shown in Figure 22.6. However, other rainfall parameters are less positively correlated. For example, the 10-min rainfall intensity appears irrelevant to flow, as shown in Figure 22.7 (Yang, 2002). Therefore, forecasting flows requires more detailed analysis.

Each rainfall parameter appears to play different roles in sub-basins of different orders in the Jiangjia Ravine. For example, according to orthogonal analysis, in first-order tributaries with a slope of 31°, the main component is initiating and antecedent rainfall, accounting for 77.6% of the variation, and the second factor is the rainfall intensity, accounting for only 2.1% of variation. However, for the main stream, antecedent rainfall accounts for 60.2%, and initiating rainfall, 39.8% of variation. Light rain can also trigger debris flows (see rainfall grade in Table 22.2 (according to National Weather Bureau)). Based on the rainfall associated with 26 debris-flow

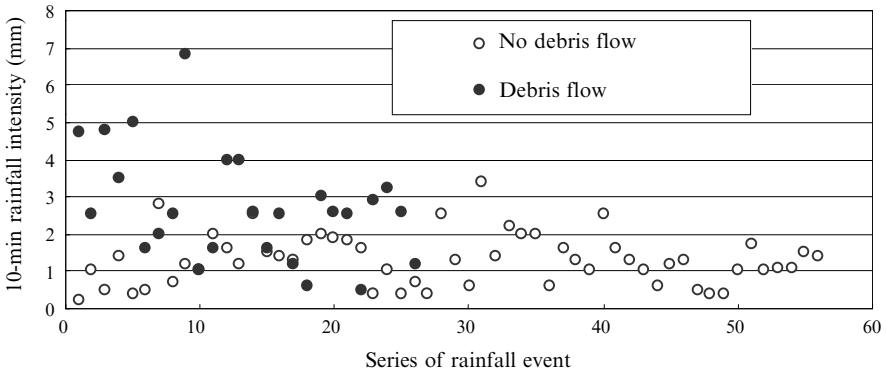

Figure 22.7. 10-min rainfall intensity and related debris flows.

Table 22.2. Rainfall grade.

Type	1-day rainfall (mm)	12-hour rainfall (mm)
Rainstorm	>50	>30
Heavy rain	25–50	15–30
Moderate rain	10–25	5–15
Light rain	<10	<5

episodes, 46.2% were caused by heavy rain, 42.3% by moderate rain, 7.7% by short-duration rain storms, and 3.8% by light rain.

In the Jiangjia Ravine, the rainfall type is also important and can be conceptually analyzed by dividing events into four types shown in Figure 22.8. A-type is concave with its rainfall intensity being smaller at first but increasing later. B-type is convex with its rainfall intensity larger at first but diminishing later. C-type is a reversed S-shape with its rainfall intensity greater first and then decreasing and finally increasing. D-type is S-shaped with its rainfall intensity varying from light to high. Each pattern is associated with a ratio or probability of the occurrence of debris flow, as listed in Table 22.3.

Of course, the minimum daily rainfall necessary to trigger debris-flow activity varies between different basins, shown by minima of 20 mm at Jiangjia Ravine, 50 mm at Heishahe Ravine in Sichuan Province, and 100 mm in Xishan at Beijing (Wu et al.,1993).

22.3 DYNAMICS

22.3.1 Velocity

The velocity field for debris flows is very difficult to measure. Accordingly the velocities provided here are values for the flow fronts which are usually turbulent

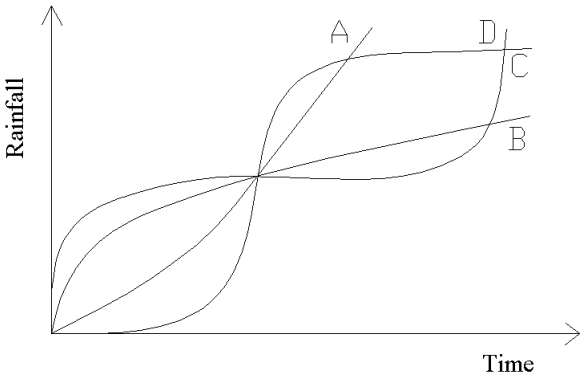

Figure 22.8. Four types of rainfall concerning debris flows in the Jiangjia Ravine.
From Yang (2002).

Table 22.3. Ratio of debris flow events under different rainfall patterns.
From Yang (2002).

Rainfall pattern	A	B	C	D	Other
Event ratio (%)	37	19	22	15	7

(Figure 22.9). In the Jiangjia Ravine, the Reynolds number of debris flows is greater than 105. The velocity at the centre of the front often exceeds 10 m/s. Turbulence varies with velocity as follows: strong turbulence (>8 m/s), turbulence (<8 m/s and >6 m/s), quasi-laminar flow (<6 m/s).

Debris flows in the Jiangjia Ravine range from hyperconcentrated flows with a density below 1.3×10^3 kg/m^3, to debris flows of various viscosities with density between 1.3×10^3 and 2.4×10^3 kg/m^3 and yield stress from 0 to 248 Pa for slurry. Viscous flow moves in the form of multiple surges, commonly followed by continuous hyperconcentrated flow. A surge usually rides on a mud layer, the so-called residual layer left by the preceding surge, which reduces resistance to flow, thus explaining why debris-flow surges move at speeds much higher than water-dominated flows under the same conditions. Compared with other locations in China, the resistance of the debris flow in Jiangjia is lower because the slurry contains a relative fine particle ratio of $d < 0.05$ mm/$d > 0.05$ mm (Rns). Experimentally, the resistance coefficient (i.e., the roughness) n_c is related to the characteristics of a debris-flow slurry by (Wang et al., 2003a):

$$n_c = 0.033 R_{ns}^{-0.51} \exp(0.34 R_{ns}^{0.17}) \ln h \tag{22.1}$$

where

$$R_{ns} = 4.59 \times 10^{-9} \eta_p^{-2.2} \exp(8.9 \times 10^{-11} \eta_p^{7.99} C_{vf}) \tag{22.2}$$

where η_p is the viscosity of slurry, C_{vf} is the volume concentration of slurry, and h is

Figure 22.9. Turbulence in a debris-flow front (the front is about 0.5 m high).
Photo: Wei, F.Q. on 19 July 2001.

depth of flow. The velocity V_{cp} can be expressed in the form of the Manning formula that is used widely in hydraulics:

$$V_{cp} = \frac{1}{n_c} h^{2/3} j^{1/2} \tag{22.3}$$

where h is the flow depth and j the gradient of the channel. Velocity on average is 5–10 m/s, with a recorded maximum of 18.2 m/s on 9 July 1998. The maximum recorded discharge is 2,914 m^3/s and five times that recorded for the trunk stream, the Xiaojiang River. The maximum annual sediment yielded from Jiangjia Ravine is 6.59×10^6 m^3.

A debris flow occurred on 25 July 1997 in the Jiangjia Ravine. The developing process was observed and the air concentration in the debris flow and its effect on flow resistance were analysed. The results are shown in Table 22.4. The air concentration appears to be closely related to the velocity, as shown in Figure 22.10, an inspection of this figure reveals that the higher the debris-flow velocity (V_{cp}), the higher the air concentration (C_a) in the flow. A relation between C_a and V_{cp} can be approximated by (Jan et al., 2000):

$$C_a = 4.2 \times 10^{-5} V_{cp}^{2.95} \tag{22.4}$$

Table 22.4. Sediment and entrained air concentrations of debris-flow samples.
From Jan, C.D. et al. (2000).

Sample No.	H (m)	V_{cp} (m/s)	C_{sa} (%)	C_s (%)	γ_{ma} (g/cm^3)	γ_m (g/cm^3)	C_a (%)
1	1.0	10.0	69.2	74.3	2.176	2.263	3.84
2	1.4	8.0	68.4	71.2	2.163	2.211	2.17
3	1.1	6.9	71.0	72.3	2.207	2.229	1.0
4	0.6	5.9	68.9	70.2	2.192	2.192	0.9

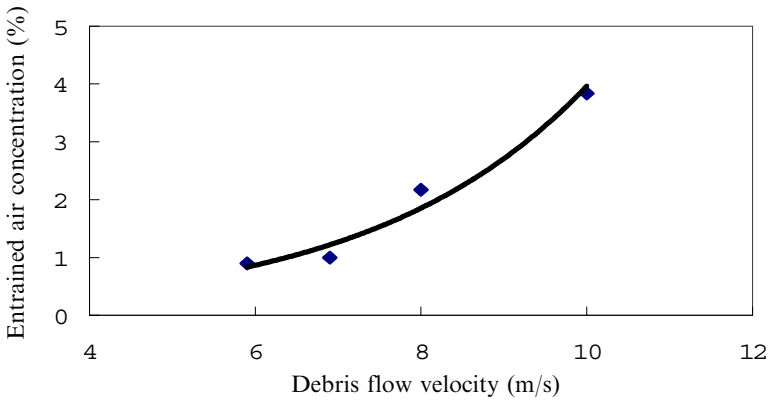

Figure 22.10. Concentration of air entrained in debris flow vs. debris-flow velocity. (Diamond symbol represents data measured from the debris-flow samples in Table 22.4; solid line represents the regression trend of these data points.)

22.3.2 Impact forces

The kinetic energy of debris flows is large because of their high material densities and velocity. When debris flows encounter some obstacles such as a pier and other constructions, the impact force can destroy these structures. In order to measure the impact forces, DDFROS constructed three rectangular, armored concrete pillars in the channel in May 1982. An electric strain sensor was installed inside a steel box in each pillar. After having recorded data from 19 flow episodes, the pillars were destroyed by debris flows in 1983. In July 1985, a new instrument, a piezo-electric crystal sensor, was put in use and measured impact forces for 40 flows. Similar tests were initiated in 2003 (Figure 22.11). The data show that debris flows impact the sensors respectively through individual stones and slurries. The stone impact is intermittent and of short duration, resulting in much greater force than the latter which is continuous and of long duration.

The two kinds of impact often concur and result in a sawtooth-shaped impulsion which is typical for most viscous debris flows. Impact interaction can continuously

Figure 22.11. Armoured concrete pillar for measuring impact force, as used in 2003. (The three steel discs in the photo are pressure sensors with 15 cm diameters.)
Photo: Hu, K.H. on 13 June 2003.

take place within the duration for as long as 500 seconds. Peaks reflect the abrupt impacts of boulders in the surge. With depths of less than 5 m and boulders smaller than 1 m in diameter, the value of dynamic pressure in this pattern is approximately 10^6 Pa. When the flow becomes more uniform, the impact shape becomes rectangular, reflecting relatively steady impact. Values range between 10^5 Pa and 10^6 Pa. The duration of peak impact is very short, usually less than 9 seconds and the maximum dynamic pressure attained is 3.0×10^6 Pa (Wu et al., 1990).

In practice the impact of the slurry is estimated as:

$$P = K\gamma_c V_{cp}^2 \tag{22.5}$$

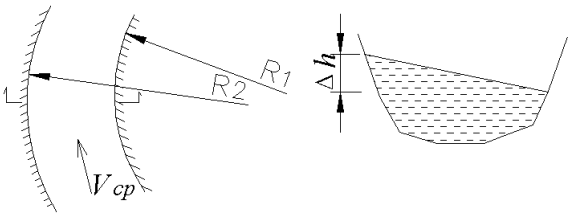

Figure 22.12. Diagram of superelevation in channel bends (see text for explanation).

where P is the dynamic pressure of debris flows, K is a coefficient (from 2.5 to 4.0), γ_c is the unit weight, and V_{cp} is velocity. For large boulders in the flow, impact P_d is:

$$P_d = \gamma_H A V_{cp} C \tag{22.6}$$

where γ_H is specific weight, A is contact area, V_{cp} is velocity, and C is transmission speed of the elastic wave impacting a rock (usually 4,000 m/s).

22.3.3 Superelevation in channel bends

A debris flow has greater inertia than common fluids. In the bends of a channel, the very large kinetic energy allows debris flows to rise to a much greater elevation than water, which often brings about extensive damage. Based on the dynamic equilibrium of a debris flow in a transverse section, the approximate formula for calculating the difference (Δh) between the surface elevations at the concave and convex banks can be written as (Kang, 1990):

$$\Delta h = 2.3 \frac{V_{cp}^2}{g} \log \frac{R_2}{R_1} \tag{22.7}$$

where V_{cp} is the velocity of the debris flow, and R_1 and R_2 are the radii of curvature for convex and concave bank, respectively. Figure 22.12 shows the meaning of each parameter.

Equation (22.7) is agreeable to the field observation. A debris flow occurred on 12 June 1973, and its parameters were determined as: $R_1 = 30$ m, $R_2 = 49.8$ m, and $C_{cp} = 8.3$ m/s. Using (22.7) we obtain $\Delta h = 3.6$ m, which is close to the measured value of 4 m.

22.4 STATIC PROPERTIES

The most fundamental static properties of debris flow are density and composition, determined by the sediment concentration in the slurry.

22.4.1 Density and concentration

Debris flows are heterogeneous. The density of the front is greater than that of the other parts of the surge because the largest clasts concentrate within the front. The

Table 22.5. Density of eight samples and their slurries from the debris flows on 8 July, 2001.

No.	Sampling time	Flow pattern	Sample (g/cm^3)	Slurry (g/cm^3) (with grain size <1.2 mm)
01-59	07:38:00	Continuous flow	1.81	1.62
01-60	08:47:20	Body of surge	1.99	1.63
01-61	09:23:41	Tail of surge	2.18	1.71
01-62	10:08:38	Tail of surge	2.22	1.69
01-63	11:38:51	Tail of surge	2.09	1.69
01-64	13:12:40	Tail of surge	1.99	1.66
01-65	14:36:55	Tail of surge	1.94	1.67
01-66	16:33:28	Continuous flow	1.71	1.54

density may change significantly within a given surge and in different surges. In a typical debris flow the first stage is a low-viscous continuous flow, followed by a viscous surge, then by a low-viscous flow, and finally by a debris flood. Different densities of flows are listed in Table 22.5 (sampled on 8 July, 2001). The density of an earlier surge body may be lower than that of a later surge tail such as in sample 01-60. The density of a highly viscous debris flow is remarkably close to the solid density of the bedrock in the Jiangjia Ravine (i.e., 2.65 g/cm^3).

Densities fall in the range between those commonly analysed in studies of sediment concentration and soil mechanics. Based on the analyses of 14 samples it was found that suspended load is related to the hydraulic strength (Wang et al., 2001):

$$C_{vt} = 0.042 f^{0.83} \tag{22.8}$$

where C_{vt} is volume concentration of suspended sediment, and f is hydraulic strength $(\gamma_c V_{cp}^3/(\rho_s - \gamma_f')\, gh\omega_0)$. The section AB in Figure 22.13 corresponds to hydraulic (dilute) debris flow.

Less viscous debris flows have properties similar to turbulent flow (hence they are called hydraulic debris flows) and subject to the same relation as in (22.8). When the sediment volume concentration is higher than 0.5, plastic features alien to the previous cases will emerge. Like debris flows of high viscosity, the viscoplastic fluid called a gravity flow has a relation as in (22.8) but with a smaller exponent after 19 samples had been analysed (Wang et al., 2001):

$$C_{vt} = 32.94 f^{0.081} \tag{22.9}$$

As shown in Figure 22.13, section BC is due to a gravity (viscous) debris flow. So the exponent in (22.8) is 10 times that in (22.9).

Table 22.6 lists typical bulk concentrations in debris flows measured at different locations at the Jiangjia Ravine.

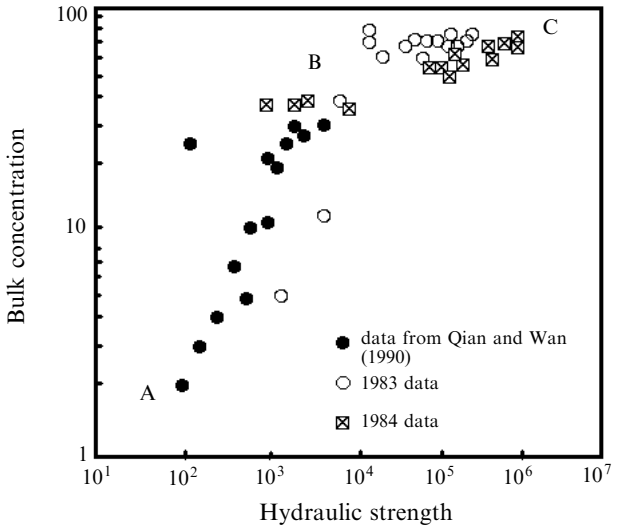

Figure 22.13. Relationship between suspended sediment and hydraulic strength.

22.4.2 Composition

Debris flows of low viscosity are characterized by similar volumes and a narrow range in grain size distribution. For example, dispersion (sorting) of particles (d_{84}/d_{16}) in a dilute debris flow in Jiangjia Ravine is from 0.01 to 0.08, and over 99% of the sediment is sand less than 2 mm in diameter, accounting for 62.5–82% of the total weight. Viscous debris flows have a wide range of grain sizes, with a dispersion of 15–40, some 500–4,000 times that of a flood flow. Grains larger than 2 mm account for 65% of the total solid weight (sand, 18.3%; clay, 18.6%) (Takahashi, 1999).

Cumulative curves of grain-size distribution show different shapes related to concentration of debris flow, reflecting variation in shear stress, cohesive force, and dispersive force of the flow (Figure 22.14). Each curve consists of two segments, representing suspended load and bedload. In the case of a viscous debris flow, this distinction becomes ambiguous, reflecting poor sorting.

As shown in Figure 22.14, eight cumulative curves may be divided into two groups. Five curves (Nos 01-60, 01-61, 01-62, 01-63, and 01-64) are much steeper than the other three in the coarse sizes. The size grading curve (Figure 22.15) has two types: single-peak such as No. 01-63, and double-peak such as No. 01-64. The grain size corresponding to the peak of size grading curve is about 20 mm for Nos 01-61–01-63 samples with greater density. The maximum peak size is 80 mm, and the minimum is 2 mm. These characteristics conform to the evolution of debris flows over time from a low-viscous continuous flow to viscous surges. The weight of grains greater than 2 mm is from 50.5–70% of viscous debris flow, with the remainder considered as fluid load that can suspend particle size up to 0.5 m. The upper limit of grain size of suspended load determines the capacity of transportation.

Table 22.6. Classification for concentration.

From Wang et al. (2001).

Categories	Classification		Density (g/cm^3)	Sediment (g/cm^3)	Porosity	Moisture (%)	Fluid limit	Flow regime	Flow character
Soil			–	–	0.19–0.44	8–11	Contract limit	Solid	
Debris flow	Viscous DF	High	2.373***	2,180.32	0.19	8.12	Plastic limit	Sub-solid	
		Middle	2.12	1,778.56	0.34	16.11	Flow limit	Laminar	Non-Newtonian flow
		Low	2.04	1,651.5	0.39	19.04			
	Subviscous DF		1.73	1,159.2	0.57	33.09	Slurry limit	Turb–laminar	
	Dilute DF		1.57 (1.24)**	906.75 (380)**	0.66	42.38	Turbid limit	Turbulence	
Hydraulics	Flood		1.17	269.96	0.90	76.09	Turbid		Newtonian flow
	Fluid		1.02	31.76	0.98	96.89	Water		

**Lower limit value; ***Upper limit value; other is mean value.

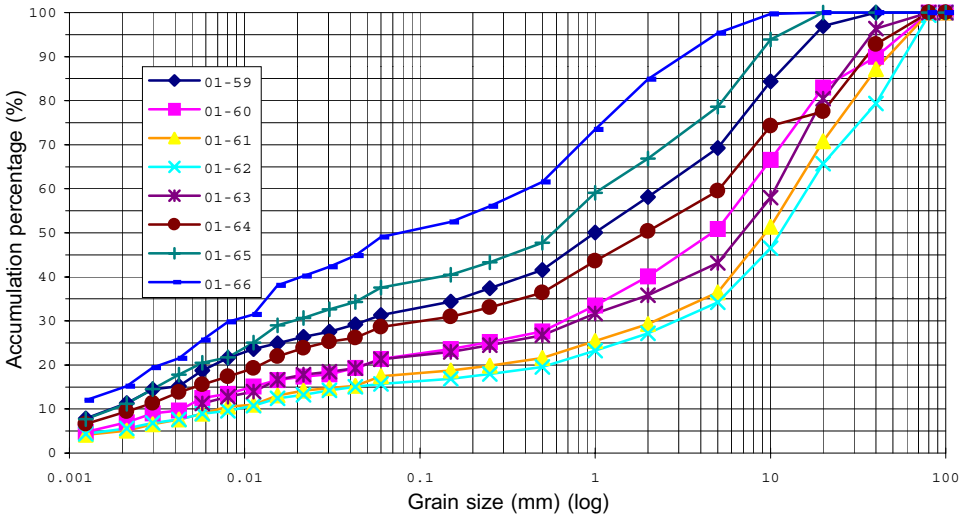

Figure 22.14. Grain-size distribution for eight debris-flow samples (8 July, 2001).

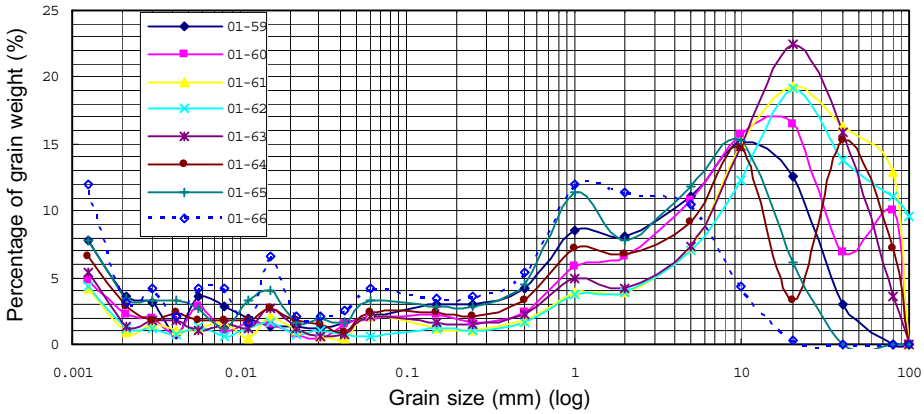

Figure 22.15. Grain weight vs. grain size for eight debris-flow samples (8 July, 2001).

Fine sediment forming the matrix of a debris flow suspends the coarser material. Sediment concentration increases as coarse grains are added and become dispersed in the matrix phase of the flow. When concentration approaches 0.5, coarse sediment can remain in suspension with relative stability. As Takahashi (1999) argued, stone flow occurs on gradient slopes between 14° and 25°. Viscous debris flows sometimes have a density as high as 2.37×10^3 kg/m^3 ($C_{vt} = 0.82$) while coarse grains typically compose 80% of the total weight of the debris flow, and can move on slopes of less than 5.7°. Different fine-grain composition for (22.1) and (22.2) in the matrix of debris flows imposes various influences on motion, flow regime, resistance, and other properties, as shown in Table 22.7.

Table 22.7. Particle size of debris flows and associated slurries, and their rheological parameters and resistance.

No.	Composition (fluid/slurry)				Slurry density (10^3 kg/m^3)	Fine ratio (R_{ns})	τ_{sf} (Pa)	η_p (Pa.s)	Slope	Mean velocity (m/s) (maximum)	Resistance
	>2 mm	2–0.05 mm	0.05–0.005 mm	<0.005 mm							
1	58	24/57	14/35	4/8	1.67	0.76	20.93	0.069	0.06–0.12	5–6	Middle
2	65.2	18.3/52	10.2/29.3	6.3/18.7	1.67	0.92	50.32	0.18	0.05–0.08	8–10 (15)	Low
3	41.1	26.7/45.3	19.0/32.3	13.2/23.4	1.57	0.81	10.91	0.041			
4	53.1	36.8/78.5	6.1/13.0	4.0/8.5	1.66	0.27	7.15	0.09	0.08–0.16	3–5 (6)	High
5	30.5	57.1/82.2	7.2/10.4	5.2/7.1	1.56	0.21	4.2	0.045			

No. 1 = debris flow of HuoShao Gully; No. 2 = viscous debris flow of Jiangjia Ravine; No. 3 = sub-viscous debris flow of Jiangjia Ravine; No. 4 = viscous debris flow of Hunshui Ravine; No. 5 = sub-viscous debris flow of Hunshui Ravine.

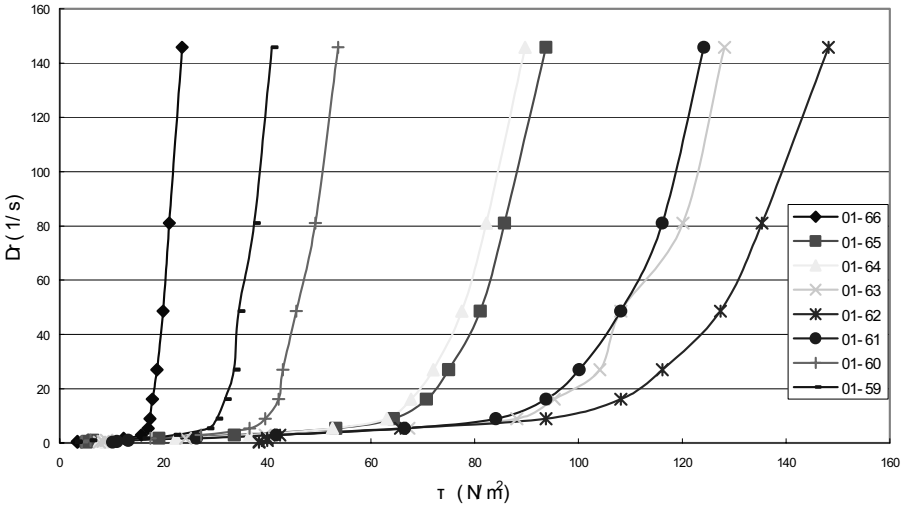

Figure 22.16. Rheological curves of debris-flow slurry samples.

Table 22.8. Yield stress and Bingham number of the slurries taken from the eight samples.

No.	01-59	01-60	01-61	01-62	01-63	01-64	01-65	01-66
Yield stress (N/m^2)	31.77	42.05	101.56	117.52	100.98	71.78	75.02	18.09
Plastic viscosity ($N.s/m^2$)	0.064	0.081	0.159	0.212	0.194	0.124	0.129	0.038

Debris flows consisting of water and fine-grained soil exhibit partial plasticity and can not be a perfect Bingham fluid. In practice, the Bingham fluid can be considered as a good approximation of sub-viscous and viscous debris flows. Generally, the yield stress of slurry in the Jiangjia Ravine is between 10 and 300 N/m^2 and the plastic viscosity between 0.4 and 15 $N.s/m^2$. Rheological curves of slurries from the eight samples above measured by a coaxial viscorator are shown in Figure 22.16. The linear least-square-approximation of the standing section of the curve gives the yield stress and plastic viscosity in Table 22.8 (Wei et al., 2002). The immediate conclusion is that yield stress and plastic viscosity increase with the density of slurry ($d_{max} = 1.2$ mm).

22.5 SEDIMENT TRANSPORTATION AND INFLUENCE ON THE MAIN RIVER

22.5.1 Sediment transportation

The annual sediment load caused by debris flows in the Jiangjia Ravine is the sum of sediment load of all the debris-flow events during a year. Debris flows commonly

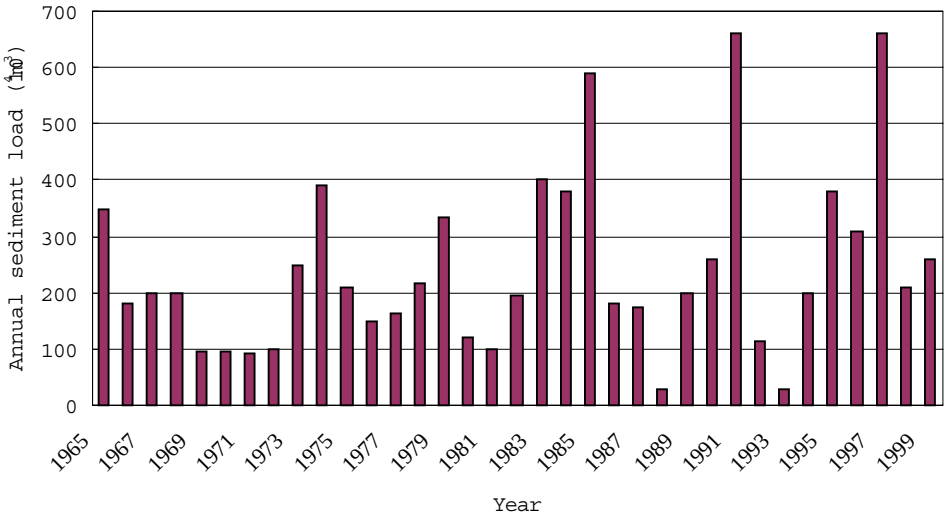

Figure 22.17. Annual sediment load caused by debris flows in the Jiangjia Ravine.
From Cui, P. et al. (1999).

Table 22.9. Sediment transporting capacity of debris flow in the Jiangjia Ravine.
From Cui, P. (1999).

				Maximum discharge and relevant parameters			
Year (Y)	Debris flow event	Flowing duration (hh:mm)	Sediment runoff annually (10^4 m^3/y)	Maximum discharge (m^3/s)	Velocity (m/s)	Sediment content (ton/m^3)	Sediment flux (ton/s)
1994	9	27:45	199.52	2,007.8	11.11	1.988	4,031.27
1995	14	68:15	373.93	1,399.7	13.33	1.847	2,585.25
1996	14	53:00	316.31	2,843.8	12.5	2.008	5,712.34
1997	18	86:21	629.28	1,341.6	12.9	1.926	2,584.59
1998	9	28:41	184.44	2,913.9	16.67	2.008	5,853.15

take place 10–20 times a year in the gully, but occurred 28 times in 1964 alone. The annual sediment loads caused by debris flows in the gully from 1965 to 1999 are shown in Figure 22.17. In the Jiangjia Ravine, 62 debris flows happened from 1994 to 1998 (Table 22.9).

Table 22.10 gives the annual sediment loads of debris flows measured in some of the gullies in China and their erosion module calculated from: $M_C = W_{CS}/A$. Debris flows in the Jiangjia Ravine have a powerful capacity for transporting sediment.

22.5.2 Influence on main river

Debris flows in the Jiangjia Ravine play a vital role in changing the nearby confluence with the Xiaojiang River through the deposition of sediment. Figure 22.18

Table 22.10. Measured annual sediment load and erosion module of debris flows in some gullies.

Gully	Catchment area A (km^2)	Measuring year	Annual sediment load W_{cs}($10^4\,m^3$)	Erosion modulus M_c($10^7\,kg/km^2a$)	Source of data
Guxiang	26.0	1964–65	461.15	47.00	Wang et al. (1984)
Liuwan	1.97	1963	9.29	12.50	Yang (1984)
Huoshao	2.03	1973	9.66	12.61	Yang (1984)
Niwan	10.3	1965	25.46	6.55	Yang (1984)
Hunshui	4.5	1976–78	63.55	37.43	Zhang and Liu (1989)
Jiangjia	45.1	1965–99	241.58	14.19	Observation
Macao	13.5	1986–88	12.35	2.42	Gao and Qi (1997)
Zhifang	3.73	1959	2.99	2.13	Lanzhou Institute of Glaciology and Cryopedology (1982)

shows one result of the confluence of a debris flow with a main channel through the laboratory simulation that was performed in the Civil Engineering Fluid Mechanics Lab of the Southwest Jiaotong University by Dr. He Yiping from October 2001 to February 2003. The set-up includes one main flume (length, 15 m; width, 0.3 m; height, 0.65 m) and one branch flume (length, 2.5 m; width, 0.1 m; height, 0.4 m). The confluence angle and discharge ratio between the main flume and branch flume are adjustable.

Following the confluence of debris flows and the main channel, the cross section and longitudinal profile of the main river will be changed nearby the confluence spot (Figures 22.19 and 22.20). The upstream profile from confluence has been elevated, and the downstream profile steepened.

On the basis of our observations and experiment, the four modes of confluence between debris flows and the main river are proposed as follows: (a) pounding the opposite bank; (b) partial-complete blockage of main channel; (c) submerging into main channel; and (d) mixing with and submerging into the main channel. Figure 22.21 shows a sketch map of the four modes.

From 4 to 12 July 2001, three episodes of debris flows occurred in the Jiangjia Ravine, which transported large amounts of sediment into the Xiaojiang River (Figure 22.22). The average discharge of the Xiaojiang River in July is between $82\,m^3/s$ and $118\,m^3/s$, in contrast with a maximum discharge of debris flow on 8 July of $775\,m^3/s$. The total volume of debris flows was $6.5 \times 10^5\,m^3$, in addition to sediment discharge of $3.4 \times 10^5\,m^3$. Figure 22.22 shows the resulting blockage. The mechanics of the confluence of debris flow with main channel is very complex

(a)

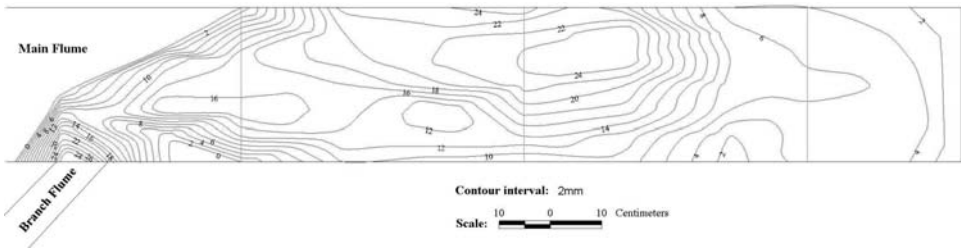

(b)

Figure 22.18. Simulation of confluence of branch and main river. (a) Snapshot of deposition after the confluence. (b) Contour map of deposition after the confluence. (The ratio of discharge per unit between the main and branch flumes is 0.354, and the confluence angle is 30°. The value in (b) is deposition thickness.)

From He (2003).

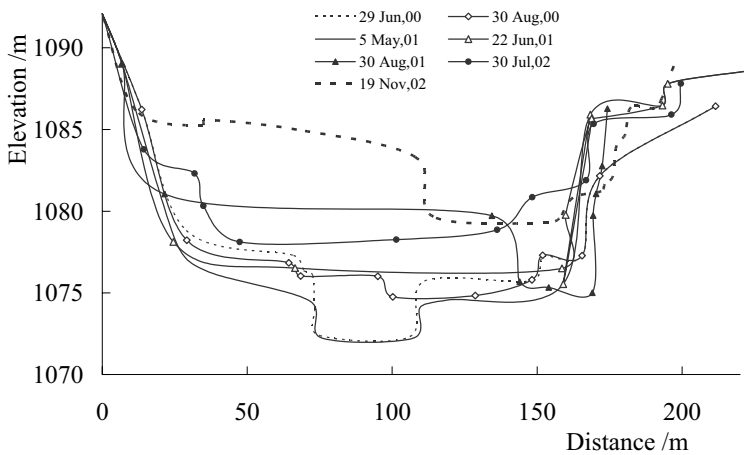

Figure 22.19. Cross section nearby the confluence spot of the Jiangjia Ravine and Xiaojiang River.

From He (2003).

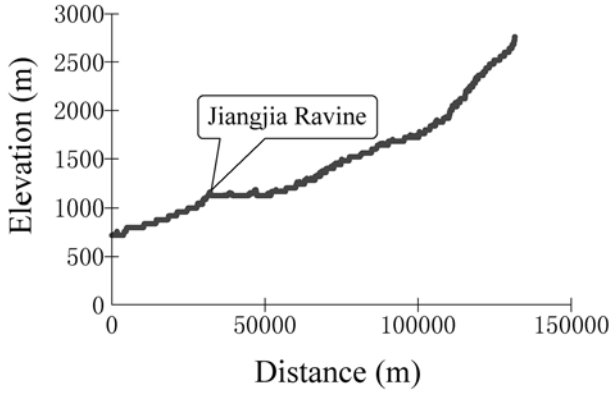

Figure 22.20. The longitudinal profile of the Xiaojiang River.
From He (2003).

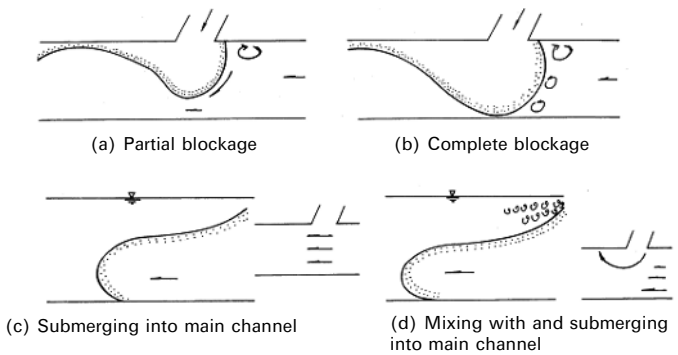

Figure 22.21. Sketch map of the four modes.
From Chen (2000).

because the debris flows are distinguished from the ambient fluid (hyperconcentrated flow) in density, composition, and viscosity. The velocity difference between the two types of fluids is high, so they are mixed, not stratified. At the confluence, we observed that debris flows slid through a short distance toward the opposite bank of the river and then were dumped into the current of the main stream. Shortly after, debris flows rolled up and down in the main channel, and a half-circular wave on the surface of the main flow produced. Upon impacting the opposite bank, the main wave divided into three separate waves. The first reversed its course in an upstream direction and disappeared; the second impacted the bank and flowed downstream; and the third ran directly downstream with a velocity exceeding that of the main flow. Pebbles and boulders were deposited near the point of confluence. The sediments resulted in the water level of the main channel rising to 8.5 m. After the dam was incised by water flow on 11 July, the river stage returned to its normal level.

(a)

(b)

(c)

Figure 22.22. Debris-flow from the Jianjgia Ravine entering the Xiaojiang River. (a) Partial blockage. (b) Complete blockage. (c) Dam break.

Photo: Wei, F.Q. on 8 July 2001.

The height of the dam was 6.5 m and the width was 301 m on that day. The resulting flood inundated fields and destroyed some buildings.

22.6 DEPOSITION

From field observations, debris-flow deposits in China can be described in terms of five classes (Cui, 1996; Scott, 1989):

1. *Normal grading*. Grains are deposited in normal order, with bigger boulders coming to rest before the smaller ones. This occurs in debris flows of lower viscosity.
2. *Disorderly graded bedding*. Grains of various diameters are randomly distributed and poorly sorted, due mainly to high viscosity.
3. *Inverse grading*. Larger grains are deposited first, occurring in the case of sub-viscous flow with a matrix with dispersive force exceeding the viscous force.
4. *Armored deposits*. Coarse sediment remains as finer material in the matrix is eroded.
5. *Basal mud deposits*. A thin layer of mud, consisting of clay and silty sands, is present at the base of the deposit.

The depositional structure of viscous debris flows is dominated by their inner speed and stress distributions. According to observational data from viscous debris flows with hyperconcentration, radical causes of formation for different graded bedding in debris-flow deposits have been analysed, using its rheological properties and the ratio of flow plug. The flow plug ratio (R_H) of the three kinds is equal to the ratio of the mean flow depth (H) to the mean flow plug (H_0), that is (Wang et al., 2003b):

$$R_H = H/H_0 \tag{22.10}$$

$$H_0 = \tau_{Bf}/(\gamma_c j g) \tag{22.11}$$

Equation (22.10) determines the speed distribution of every kind of viscous debris flow and total depth condition development by a flow plug of Bingham fluid. That can approach to characteristics of graded bedding texture of every kind for viscous debris flow.

For coarse gravel to deposit disorderly formed hybridize graded bedding structure, because of action of inside resistance by high-viscous medium. It is most graded bedding deposit of viscous or high-viscous debris flow with $R_H = 12$. These deposit structures are observed in many ravines. But when the mean flow plug ratio is high, about 100 in sub-viscous debris flow, there is a lower structure substantial degree (C_{vt}/C_{vm}) for 0.85. So that there are dispersive force and viscous force together in the sub-viscous debris flows, or dispersive force is more than viscous force in sub-viscous debris flow. There is inversely graded bedding structure after debris-flow deposit. There are the structures in most lahar deposits in America, Japan. And similar structures are found in some deposits in China, for example of Dawazhi dully in the branch of Jiangjia Ravine.

When the mean flow plug ratio is about 20–22 in viscous debris flow, they would form the bedding structure of the gravel accumulated at surface, which are the same geomorphologic phenomenon in Major's experiment (Major, 1994). Here that is specially emphasized that the gravel in squirm condition of hyperconcentration viscous flows would tend to upward motion for the effect of Weissenberg, namely viscoplastic principal strain difference, and they are different from rough bedding structure (Wang et al., 2003b).

22.7 HAZARD MITIGATION

Measures for mitigating debris-flow hazards include protective engineering works, forecasting and warning systems allowing for emergency education, and land-use regulation and zoning, as well as evacuating and emergency.

22.7.1 Structured mitigation

Check dams of various types are used in source areas to stabilize slopes, to control channel erosion, and to trap coarse debris. Armored channels are used in downstream areas to convey flows to trunk streams without damaging villages, roads, and fields. Several types of check dams, channels, and structures have been engineered to reduce the damage from debris flows in China. Finally, structures in deposition areas may be required to protect specific facilities. Figure 22.23 shows several main check dams and channels in the Dongchuan area.

A systematic plan for debris-flow prevention has been carried out in the Jiangjia Ravine (Wu et al., 1990). The main engineering works were designed for the upper area – Duozhao gully and lower sections of the ravine (Figure 22.24). In the Duozhao gully, 117 check dams were constructed in the 1980s in order to stabilize slopes and prevent tributaries from incising, and they trap up to $7 \times 10^5\,m^3$ of sediment. Most matter came from the Duozhao gully before the 1980s, but after 1985 most of the matter came from the Menqian gully and the mean debris-flow scale decreased.

In the lower reaches of the Jiangjia Ravine, drainage grooves of 1,800 m in length were designed to protect villages and farmland, as well as to control and spread deposition in order to maximize the potential for the subsequent use for rice cultivation. About $0.2\,km^2$ in the ravine was planted to restore the vegetation cover.

Debris flows often occur in areas of poor vegetation cover, and restoration of that cover can be effective in reducing debris-flow activities. Measures include forestation, returning cultivated land to forest, banning herding in grasslands, and a combination of these approaches.

Great benefits were obtained from these disaster reducing works. The main benefits include control of debris-flow disasters, recovering ecological environment, reclaiming $7 \times 10^5\,m^2$ of farmland, and protecting two bridges and a factory in the upper part of the Xiaojiang river, and so on.

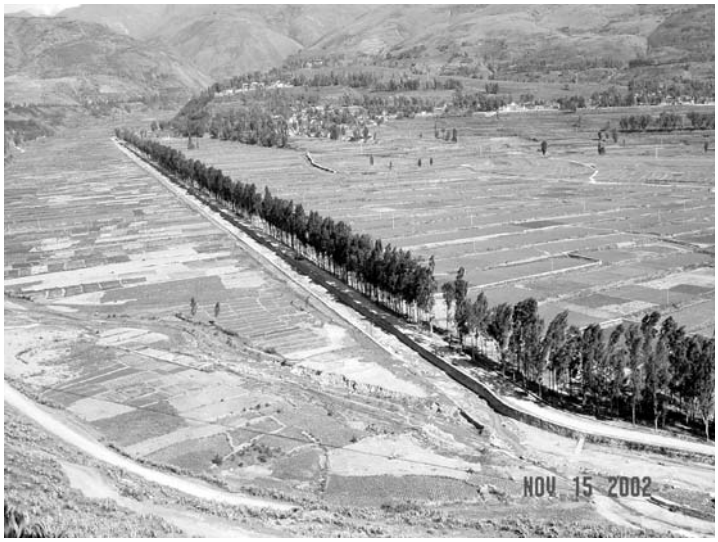

(a)

(b)

Figure 22.23. Two types of drainage groove. (a) Ladder-shaped groove. (b) V-shaped groove.

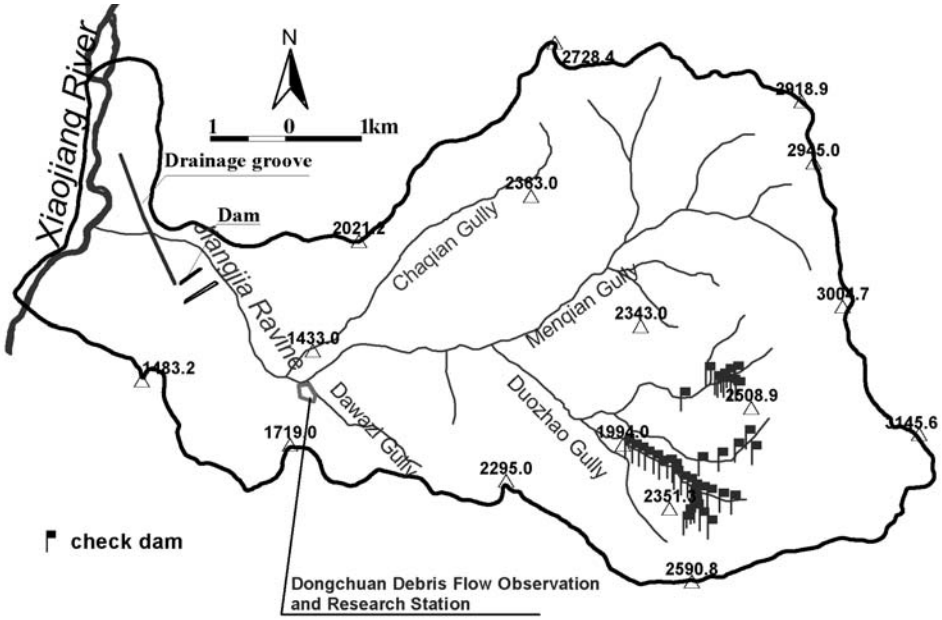

Figure 22.24. Main structure mitigation in the Jiangjia Ravine.

22.7.2 Forecasting and warning system

Debris flow occurs in response to rainfall, so we focus our forecasting on monitoring and forecasting threshold levels of rainfall. Despite the fact that no direct quantitative relation has been found between flow occurrence and precipitation, empirical formulas can estimate critical conditions at which debris flows occur. For instance, one can roughly tell that a debris flow is probable when antecedent and concurrent rainfall intensity reach a certain value. This method is limited by its oversimplification.

On the other hand, the warning system installed in the Jiangjia Ravine functions very well, which includes Acoustic Flow Monitors (AFMs) that function as seismometers; ultrasonic detectors; and infrasound sensors. AFMs sense frequencies ranging from 0.2–1,000 Hz. Signals received and processed by computer can be used to trigger a warning alarm in advance of a debris flow, the delay time being:

$$T = (S_2 - S_1)/V_{cp} \tag{22.12}$$

where V_{cp} is the mean velocity of the debris flow and $(S_2 - S_1)$ is the distance between the observation sections. Ultrasonic detectors are used because flow depth is typical of the flow magnitude and possible damage, and can give a telemetered alarm 10 km from the source of the debris flow.

In practice, an ultrasonic signal is triggered by a debris flow at its initiation in the source area. The velocity of the ultrasonic wave is about the same as that of audible

sound in air (i.e., about 344 m/s at 20°C), much faster than the velocity of a debris flow. Hence, it can warn of the arrival of a debris flow before the flow reaches the lower parts of the gully, if we have a device to receive the wave. The infrasonic observation system for debris flows (Zhang, 2003) has been designed and developed.

22.8 CONCLUSIONS

The Jiangjia Ravine provides most excellent conditions for investigating debris flows. In the last 40 years, scientists from the Institute of Mountain Hazards and Environment, Chinese Academy of Science, have kept observing and monitoring debris-flow occurrences for their formation, motion, deposition, and their action on local landforms and environments. The most conspicuous features of debris flows and their related studies in this very basin are as follows:

1. Debris flows occur at rather high frequencies and have averaged 11 events per year during the last 40 years, allowing long-term and systematic observations to some extent parallel to observations of climate and hydrology, which have been supposed to be interrelated with debris flows.
2. Each debris-flow event in the Jiangjia Ravine consists of tens to hundreds of surges, providing a wide variety of phenomena that are rarely seen in other areas of the world. This calls for systematic research on debris flows.
3. The Jiangjia Ravine has provided an ideal site to explore debris-flow formation and initiation in combination with a background of loose materials and rainfall. This is significant for debris-flow forecasting.
4. Observation data and videos of living debris flows in the Jiangjia Ravine are the most unique resource open to future studies in the field.

22.9 ACKNOWLEDGEMENTS

The authors are grateful to Dr. Scott and Dr. Jakob for their help in reviewing the draft and also to the Dongchuan Debris Flow Observation and Research Station, Chinese Academy of Sciences, for permission to use data and pictures. Dr. James Gardner of the University of Manitoba, Canada, assisted in editing the paper. This research is partly supported by the Chinese Science Foundation for Outstanding Youth (Grant No. 40025103) and National Science Foundation of China (Grant No. 4P831010).

22.10 REFERENCES

Chen, D.M. (2000) Mechanism of confluence between debris flow and the main river. PhD thesis, Chinese Academy of Water Conservancy Science [in Chinese].

Cui, P. (1999) Impact of debris flow on river channel in the upper reaches of the Yangtze River. *International Journal of Sediment Research*, **14**(2), 201–203.

Cui, P., Wei, F.Q., and Li, Y. (1999) Sediment transported by debris flow to the lower Jiansha River. *International Journal of Sediment Research*, **14**(4), 67–71.

Cui, Z.J. (1996) *Debris-flow Deposition and Environment* (p. 192). Ocean Press, Beijing [in Chinese].

Gao, S.Y. and Qi, L. (1997) Characteristics of debris flow in Macao Gully in Wudu County, Gansu Province. *Mountain Research*, **15**(4), 300–304 [(in Chinese].

He, Y.P. (2003) Influence of debris flow on river channel change of mountains. PhD thesis, Chinese Academy of Science [in Chinese].

Jan, C.D., Wang, Y.Y., and Han, W.L. (2000) Resistance reduction of debris flow due to air entrainment. In: G.F. Wieczorek and N.D. Naeser (eds), *Debris-flow Hazards Mitigation: Mechanics, Prediction, and Assessment: Proceedings of the 2nd International Conference on Debris-flow Hazards Mitigation, Taiwan*. A.A. Balkema, Rotterdam.

Kang, Z.C. (1990) *Motion Characteristics of Debris Flow at Jiangjia Gully, Yunnan Province, China*. International Research & Training Center on Erosion & Sedimentation.

Lanzhou Institute of Glaciology & Cryopedology, Traffic Science Institute of Gansu Province (1981) *Debris Flow in Gansu Province* (pp. 83–85, 114–115). Publishing House of People's Transportation, Beijing [in Chinese].

Li, J. and Wu, J.S. (1980) Dynamical data of debris flow in Jiangjiagou Gully (Unpublished) [in Chinese].

Major, J.J. (1994) *Experimental Studies of Deposition at Debris Flow Flume* (USGS Open-file Report 1-28). US Geological Survey, Reston, VA.

Qian, N. and Wan, Z.H. (1990) *Sediment Kinematics*. Science Press, Beijing [in Chinese].

Scott, K.M. (1989) *Origins, Behavior and Sedimentology of Lahars and Lahar Run-out Flows in the Toutle Cowlitz River System, Mt. St. Helens* (USGS Publication PPA19). US Geological Survey, Reston, VA.

Takahashi, T. (1999) Mechanics of viscous debris flow. In: *China–Japan Joint Research on the Mechanism and the Countermeasures for Viscous Debris Flow* (pp. 119–125). Institute of Mountain Hazards & Environment, CAS, and Disaster Prevention Research Institute, Kyoto University.

Tang, B.X., Zhou, B.F., and Wu, J.S. (2000) *Debris Flow in China* (pp. 1–10). Commercial Press, Beijing [in Chinese].

Wang, Y.Y., Jan, C.D., Han, W.L., Hong, Y., and Zhou, R.Y. (2003a) Stress-strain properties of viscous debris flow and determination of velocity parameter. *Chinese Journal of Geological Hazard and Control*, **14**(1), 9–13 [in Chinese].

Wang, Y.Y., Jan, C.D., Han, W.L., and Zhou, R.Y. (2003b) A study on the forming mechanism of the bedding structure of gravel accumulated at the surface, and rough bedding structure in deposits of viscous debris flows with hyperconcentration. *Acta Sedimentologica Sinica*, **21**(2), 205–210 [in Chinese].

Wang, Y.Y., Jan, C.D., and Yan, B.Y. (2001) *Debris Flow Structure and Rheology*. Hunan Science and Technology Press, Changsha, China [in Chinese].

Wang, W.J., Zhang, S.C., and Wang, J.Y. (1984) *Characteristics of Glacial Debris Flow in Guxiang Gully, Tibet Autonomous Region* (Memories of Lanzhou Institute of Glaciology & Cryopedology, pp. 18–34). Chinese Academy of Science, Beijing, and Science Press, Beijing [in Chinese].

Wei, F.Q., Hu, K.H., Cui, P., Chen, J., and He, Y.P. (2002) Mechanism of blocking of Xiaojiang River by debris flow of Jiangjiagou Gully. *Journal of Water and Soil Conservation*, **16**(6), 71–75 [in Chinese].

Wu, J.S., Kang, Z.C., Tian, L.Q., and Zhang, S.C. (1990) *Debris Flow Observation and Research in Jiangjiagou Ravine, Yunnan*. Science Press, Beijing [in Chinese].

Wu, J.S., Tian, L.Q., Kang, Z.C., Zhang, S.C., and Liu, J. (1993) *Debris Flow and Its Comprehensive Control*. Science Press, Beijing [in Chinese].

Yang, K. (2002) Relationship between debris flow and precipitation in Jiangjiagou Gully. MSc thesis, Chinese Academy of Science [in Chinese].

Yang, Z.N. (1984) *Viscous Debris Flow in Wudu Prefecture and Estimation of Their Basic Parameters* (Memories of Lanzhou Institute of Glaciology & Cryopedology, pp. 22–25). Chinese Academy of Science, Beijing, and Science Press, Beijing [in Chinese].

Zhang, S.C. (2003) Detecting infrasound emission of debris flow for warning purposes. In: D. Rickenmann and C-L. Chen (eds), *Debris-flow Hazards Mitigation: Mechanics, Prediction, and Assessment*. Millpress, Rotterdam.

Zhang, X.B. and Liu, J. (1989) *Debris Flow in Dayingjiang Basin, Yunnan Province* (pp. 103–103). Chengdu Cartography Press, Chengdu, China [in Chinese].

Zhang, X.B. and Liu, J. (1989) *Debris Flow in Dayingjiang Basin, Yunnan Provinces* (pp. 103–107). Chengdu Cartography Press, Chengdu, China [in Chinese].